Decadal Changes of Wind Stress over the Southern Ocean Associated with Antarctic Ozone Depletion

XIAO-YI YANG

Key Laboratory of Tropical Marine Environmental Dynamics, South China Sea Institute of Oceanology, Chinese Academy of Sciences, Guangzhou, China

RUI XIN HUANG

Department of Physical Oceanography, Woods Hole Oceanographic Institution, Woods Hole, Massachusetts

DONG XIAO WANG

Key Laboratory of Tropical Marine Environmental Dynamics, South China Sea Institute of Oceanology, Chinese Academy of Sciences, Guangzhou, China

(Manuscript received 19 April 2006, in final form 15 September 2006)

ABSTRACT

Using 40-yr ECMWF Re-Analysis (ERA-40) data and in situ observations, the positive trend of Southern Ocean surface wind stress during two recent decades is detected, and its close linkage with spring Antarctic ozone depletion is established. The spring Antarctic ozone depletion affects the Southern Hemisphere lower-stratospheric circulation in late spring/early summer. The positive feedback involves the strengthening and cooling of the polar vortex, the enhancement of meridional temperature gradients and the meridional and vertical potential vorticity gradients, the acceleration of the circumpolar westerlies, and the reduction of the upward wave flux. This feedback loop, together with the ozone-related photochemical interaction, leads to the upward tendency of lower-stratospheric zonal wind in austral summer. In addition, the stratosphere–troposphere coupling, facilitated by ozone-related dynamics and the Southern Annular Mode, cooperates to relay the zonal wind anomalies to the upper troposphere. The wave–mean flow interaction and the meridional circulation work together in the form of the Southern Annular Mode, which transfers anomalous wind signals downward to the surface, triggering a striking strengthening of surface wind stress over the Southern Ocean.

1. Introduction

More and more evidence shows that anthropogenic influence is an important cause of recent climate changes. The discovery of dramatic seasonal ozone loss in the Antarctic is a good example. According to the heterogeneous chemistry theory proposed by Crutzen and Arnold (1986), McElroy et al. (1986), and Solomon et al. (1986), chlorine- and bromine-catalyzed photochemical reactions destroy most of the stratospheric ozone in the Antarctic region. The increasing content of atmospheric chlorine produced by human activities, therefore, has been identified as a crucial player for the springtime ozone hole that developed in the late 1970s (Solomon 1999; Albritton et al. 1998).

Many studies have discussed the impacts of severe Antarctic ozone depletion on global climate change. Randel and Wu (1999) documented a steplike cooling during Antarctic spring in the lower stratosphere, which can be explained through model simulations as a radiative response to the observed ozone loss (Shine 1986; Mahlmann et al. 1994; Langematz 2000). Ramaswamy et al. (2001) concluded that more than three-quarters of the trend in lower-stratospheric temperature over the period 1979–90 may be attributed to ozone depletion. Observations indicate that the Antarctic vortex has strengthened over recent decades (Waugh et al. 1999; Zhou et al. 2000). Thompson and

Corresponding author address: Xiao-Yi Yang, Key Laboratory of Tropical Marine Environmental Dynamics, South China Sea Institute of Oceanology, Chinese Academy of Sciences, 164 West Xingang Road, Guangzhou 510301, China.
E-mail: yxy@scsio.ac.cn

DOI: 10.1175/JCLI4195.1

Solomon (2002, hereafter TS02) argued that photochemical ozone loss may be the main external forcing responsible for driving this trend, the high polarity of the Southern Annular Mode (SAM), and the most significant tropospheric trends. Through numerical simulations, Gillett and Thompson (2003, hereafter GT03) further discussed the impacts of Antarctic ozone loss upon climate at the earth's surface and in the stratosphere.

At present, however, the dynamics of Antarctic ozone depletion and its climatic implication are far from being resolved, partly due to the complicated interplay between Antarctic ozone and other climate variables, as well as the indistinct stratosphere–troposphere coupling processes.

This study is mainly motivated by Huang et al. (2006), who found that the wind energy input to the Antarctic Circumpolar Current (ACC) increased remarkably during recent decades. Since wind energy input to the ocean is the primary source of external mechanical energy driving the oceanic general circulation (Huang 1998, 2004; Wunsch and Ferrari 2004), this inspires us to explore the causes of the decadal change of the surface wind stress over the Southern Ocean.

In our discussion of Southern Hemisphere (SH) climate phenomena, we define austral spring as September–November, austral summer as December–February, and so on. We define an "austral year" as beginning on 1 July.

In this work, we present evidence to demonstrate the following:

1) The positive trends of surface wind stress over the Southern Ocean (45°~60°S) exhibit strong seasonality with the peak in austral summer (January).
2) This trend is closely related to the spring Antarctic ozone depletion.
3) There exists an ozone-related thermodynamic and dynamical feedback mechanism in the lower stratospheric Antarctic. The resulting anomalous wind can propagate downward to the surface through the SAM-related wave–mean flow interaction and meridional circulation.

The outline of the work is as follows: The data and methods applied are introduced in section 2. In section 3a, the time series and trends of Antarctic ozone and wind stress over the Southern Ocean are presented, including the variability in their seasonal cycles. Then we describe the lower-stratospheric circulation variation associated with Antarctic ozone depletion in section 3b. Next, the downward propagation of zonal-wind anomalies is described in section 3c. Finally, section 4 presents the conclusions and discussion.

2. Data and analysis technique

Some studies have indicated a deficiency of National Centers for Envrionmental Prediction–National Center for Atmospheric Research (NCEP–NCAR) reanalysis data in representing the long-term climate change at high and midlatitudes of the Southern Hemisphere (Hines et al. 2000; Marshall 2002, 2003). The problem arose from the assimilation of the Australian Surface Pressure Bogus Data (PAOBS) for the SH in which the observations were erroneously shifted by 180° in longitude, affecting the period 1979–92. Marshall (2003) suggested that compared with NCEP–NCAR reanalysis data, the 40-yr European Centre for Medium-Range Weather Forecasts (ECMWF) Re-Analysis (ERA-40) dataset provides an improved representation of SH high-latitude atmospheric circulation variability. As a result of satellite data assimilation after 1978 and a higher level of skill, ERA-40 is superior to the NCEP–NCAR dataset for the research of long-term climate change in the SH extratropics. Therefore, the ERA-40 monthly dataset is chosen in this study.

Two monthly SAM indices are used in this study: the first one is a station-based index following the methodology of Marshall (2003); the second one is derived by applying EOF analysis to the 18-level SH extratropical geopotential height field [weighted by the square root of the cosine of latitude, following Chung and Nigam (1999)] and taking respective time series of leading modes as the SAM indices [similar to the method of Thompson et al. (2005)].

To test the reliability of the trend analyses based on the ERA-40 data, we also use other in situ observations and satellite measurements, including the monthly surface wind speed at Macquarie Island (54.5°S, 158.9°E) from the Australian Government Bureau of Meteorology, Special Sensor Microwave Imager (SSM/I) satellite wind speed data, Total Ozone Mapping Spectrometer (TOMS) monthly total column ozone data, and South Pole CO_2 data.

The linear trend is estimated as the linear regression coefficient of each grid point data on time. The significance level of trend is tested by applying the *t*-test method of Santer et al. (2000). Given the highly zonal symmetry of the SH atmospheric circulation, the trend estimation and other analyses in this study are all based on zonal-mean data.

The wind stress field is calculated from the 10-m U wind and V wind, using the bulk formula, $\boldsymbol{\tau} = \rho_0 C_D |\mathbf{V}| \mathbf{V}$, where $\boldsymbol{\tau}$ and $\mathbf{V}$ denote the wind stress vector and 10-m wind vector, respectively; $|\mathbf{V}|$ the wind speed at 10 m; and ρ_0 the air density. The drag coefficient C_D

is calculated from the empirical formula (Garratt 1977), $C_D = 7.5 \times 10^{-4} + 6.7 \times 10^{-5} \times |\mathbf{V}|$.

The Eliassen–Palm (EP) flux is computed from daily wind and temperature fields, using the following formula in spherical coordinates:

$$F_\lambda = -\frac{2\pi R^2 \cos^2(\phi)}{g}[U^*V^*];$$

$$F_p = -\frac{2\pi R^3 \cos^2(\phi)}{g} f[V^*\theta^*](\partial\theta_S/\partial p)^{-1};$$

where R is the earth's radius, g is the gravity, f the Coriolis parameter, ϕ is latitude, θ denotes potential temperature, and θ_s the global mean potential temperature on a pressure surface. Note that to facilitate straightforward physical interpretation we have added a minus sign for the vertical component of the EP flux for the Southern Hemisphere so that the positive value of vertical EP flux represents the upward wave forcing and poleward eddy heat flux. For the similar purpose, the Ertel's potential vorticity (PV) in the SH is defined as (without the minus sign in the front)

$$P = g(f + \zeta_\theta)\left(\frac{\partial\theta}{\partial p}\right).$$

3. Results

a. Wind stress trend and its seasonality

Figure 1 shows the various normalized time series and their linear trends. The trends are calculated for two distinct periods: prior to 1980 and 1980–99. For clarity, trend coefficients are presented in Table 1, with the bold phase and asterisk denoting the trends above the 95% significance level t test. It is clear that for the zonal wind stress (Taux) over the Southern Ocean (45°–60°S; Fig. 1a), the positive trend is statistically significant for the period 1980–99 only (Table 1). Although the ERA-40 dataset is preferred to the NCEP–NCAR dataset for long-term climate study, cautions must be taken in that ERA-40 data is also dominated by model simulations in SH prior to 1979 (Bengtsson et al. 2004). As the satellite measurements have been assimilated since the late 1970s, the statistical results of climate change may be simply due to the data discrepancy in assimilation process for the pre- and post-1980 periods. Therefore, the comparison of ERA-40 data and in situ observation time series is needed to verify the trend analysis. Both in situ observations (Fig. 1b) and satellite measurements (Fig. 1c) have significant upward trends after the 1980s, and the Macquarie wind speed trends are almost twice as much as those of the ERA-40 zonal wind stress for the whole 40 years (see Table 1). In addition, linear correlation analysis indicates the consistency of Macquarie observations and ERA-40 wind stress, the correlation coefficients being as high as 0.466 for the period from January 1958 to December 2001 (528 months). This confirms the robustness of ERA-40 trends analysis. The Marshall SAM index (Fig. 1d) and the Antarctic (60°S poleward averaged) total column ozone data (Fig. 1e for ERA-40 and Fig. 1f for TOMS satellite data) also exhibit significant trends after the 1980s, though the ozone trend is much more pronounced than that of the SAM.

The seasonality of surface wind stress during 1980–2000 is delineated by calculating respective zonal-mean zonal (Fig. 2a) and meridional (Fig. 2b) wind stress trends and Ekman pumping trends (Fig. 2c) for each calendar month. We see that all three variables exhibit strong seasonality in their trends at midlatitudes, with the strongest trends occurring in January. Secondary peaks with marginally significant trends appear in May. More specifically, the zonal and meridional wind stress trends in January are characterized by dipolelike patterns with the nodal latitude of ~47.5°S, which, by referring to the climatology (figures omitted), implies a strengthening of westerly and southerly wind stresses poleward of 47.5°S and slight weakening equatorward of 47.5°S. As for the region of our interest—the Southern Ocean (45°–60°S)—we see an overall upward trend of both wind stresses and Ekman pumping rate, and a poleward drift of the centers of maximum wind stress.

Previous studies showed that the Antarctic ozone depletion culminates during spring [e.g., in situ observations by Farman et al. (1985) and satellite measurements by Stolarski et al. (1986)]. The linear trend analysis of ERA-40 Antarctic (60°–90°S) total column ozone also shows a strong seasonality (Fig. 3a) with the peak centered in austral spring (September–November). The seasonality in linear trend analyses suggests a possible linkage between the strengthening of wind stress over the Southern Ocean in summer and the spring Antarctic ozone depletion. However, ozone depletion mainly occurs in the lower stratosphere. How could ozone depletion in the lower stratosphere drive the surface wind stress change with a lag of 1~2 months? This question deserves further investigation.

b. The interannual variability and long-term trend of the lower-stratospheric circulation associated with spring Antarctic ozone depletion

Since the ERA-40 ozone data assimilates both the TOMS total ozone and solar backscatter ultraviolet (SBUV), ozone profile (Kallberg et al. 2004), the monthly correlation between TOMS Antarctic ozone (Fig. 1f) and ERA-40 Antarctic ozone (Fig. 1e) is as

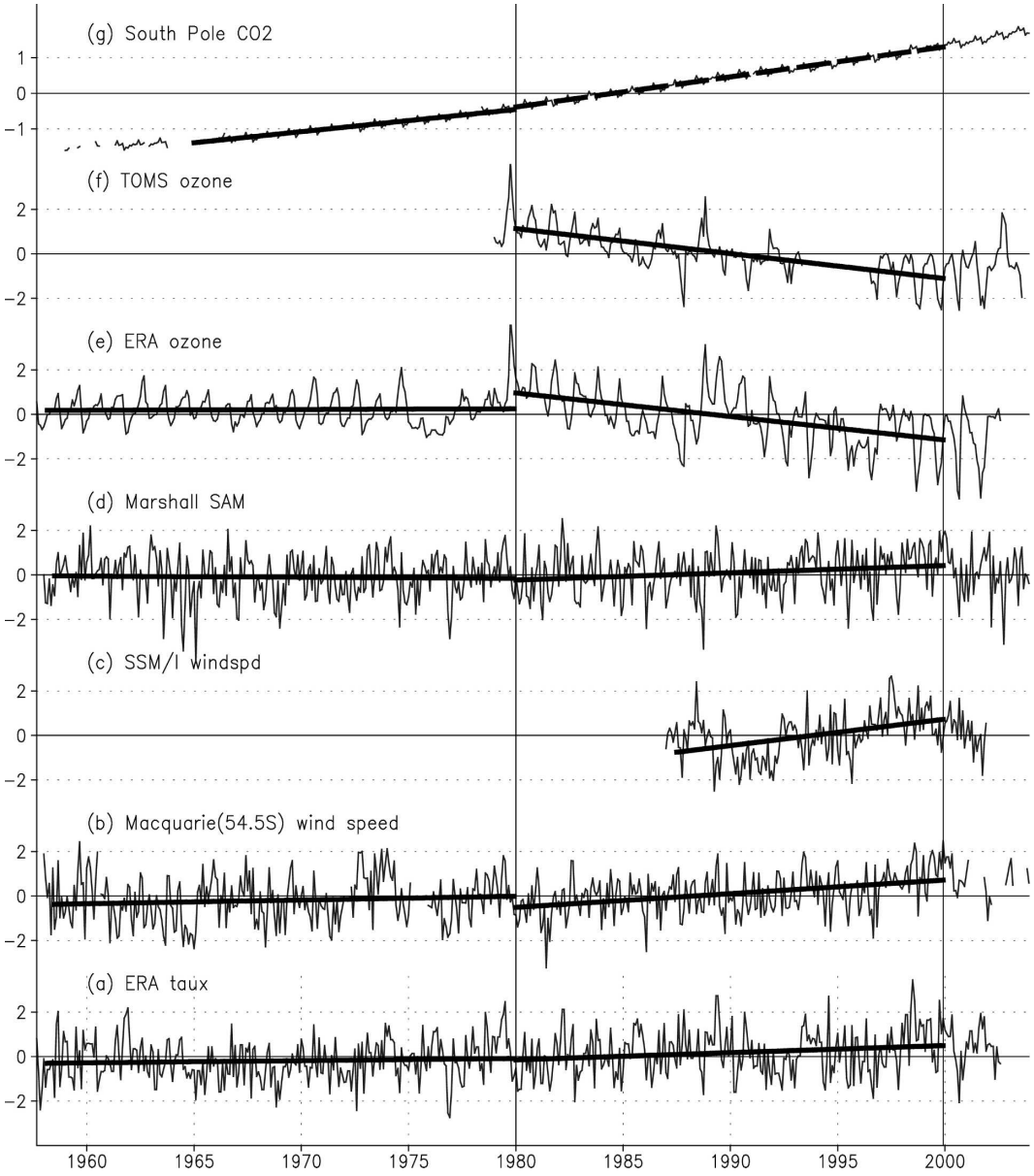

FIG. 1. Normalized time series (thin line) and their linear trends (thick line): (a) ERA-40 zonal wind stress over the Southern Ocean (45°–60°S), September 1957–August 2002; (b) in situ observations of wind speed at Macquarie Island (54.5°S, 158.9°E), January 1958–December 2003; (c) the SSM/I satellite wind speed data, January 1987–December 2001; (d) the Marshall Southern Annular Mode index based on the observational SLP data, January 1958–December 2003; (e) ERA-40 Antarctic (60°–90°S) total column ozone, September 1957–August 2002; (f) TOMS satellite Antarctic (60°–90°S) total column ozone, January 1979–December 2003; and (g) atmospheric CO_2 concentrations at South Pole (89°59′S, 24°48′W), September 1957–December 2003. (Note that all trends are calculated from a 13-month running mean of respective time series, which can reduce the sensitivity of trend value to marginal effects. Two separate periods: pre-1980 and January 1980–December 1999 are chosen for the linear trend analysis.)

high as 0.801 for the period January 1979–December 2003. A spring Antarctic ozone depletion index (SAODI) is constructed by taking the normalized ERA-40 spring (September–November) minus the averaged total column ozone over the Antarctic region. Figure 3b shows the time series of SAODI. Here the time series is multiplied by −1 so that the positive trend of the index denotes ozone depletion.

The interannual variability associated with spring Antarctic ozone losses is diagnosed by lag-regressing

TABLE 1. Linear trend coefficients of the various time series as listed in Fig. 1 (trends above the 95% *t*-test significance level are denoted by boldface).

	Data source	Pre-1980 (month^{-1})	Post-1980 (month^{-1})
Zonal wind stress (Taux)	ERA	0.000 82	**0.002 68**
Wind speed	Macquarie station	0.001 40	**0.005 11**
	SSM/I	—	**0.009 91**
SAM index	Marshall SLP (observation based)	−0.000 41	**0.0027**
Ozone	ERA	0.000 28	**−0.008 81**
	TOMS	—	**−0.009 35**
CO_2	In situ (South Pole)	**0.005 19**	**0.007 05**

the climate variables onto the SAODI for the same austral year (from July to next June; Fig. 4). Owing to Antarctic ozone loss in spring, the Antarctic (60°–90°S) stratospheric geopotential height drops (Fig. 4a) and the Antarctic lower stratosphere–tropopause cools (Fig. 4b) in spring and summer. The most dramatic changes occur in November in the lower stratosphere and December at the tropopause, one or two months after the peak of the Antarctic ozone hole. The results of regression analysis presented here are essentially consistent with results from a model forced by prescribed stratospheric ozone depletion (GT03, their Fig. 2). Nevertheless, some discrepancy exists in the troposphere. The tropospheric responses to spring Antarctic ozone depletion are insignificant in our study (in contrast to that of GT03), which implies that the linkage between stratospheric ozone depletion and tropospheric variability is indirect. This necessitates a careful examination of the stratosphere–troposphere coupling processes.

The latitude–altitude cross sections of ozone-induced temperature variability (Figs. 5a,b) reveal that cooling of the polar region parallels warming of the subtropics in the lower stratosphere, resulting in an enhancement of the meridional temperature gradient. Through the thermal wind relation, this leads to strengthening of the zonal wind shear in the midlatitude lower stratosphere (Fig. 4c). To further expound the dynamical consequence of the Antarctic ozone depletion, we carried out linear regression analyses of the Antarctic Ertel's PV related to SAODI. Spring Antarctic ozone depletion is accompanied by significant changes in Antarctic potential vorticity in spring and summer (Fig. 4d). It is readily seen that, when the Antarctic ozone depletion occurs, PV at the Antarctic tropopause (200 hPa) decreases and PV in the middle and lower stratosphere increases. As the increase of PV at high latitudes means the strengthening of the SH polar vortex, this pattern implies a stronger and more isolated polar vortex in a lower stratosphere level in late spring/early summer. The result is essentially consistent with many previous studies (e.g., Hartmann et al. 2000; Thompson et al. 2000; Baldwin et al. 2003b), which established the connections between polar vortex, polar night jet, and stratospheric ozone loss.

To expound on the PV dynamics associated with the ozone hole, variability in the correlation between SAODI and zonal-mean PV is presented for two typical months: November (Fig. 5c) and December (Fig. 5d). These two months are chosen to represent the instant and prolonged effects of spring Antarctic ozone depletion. The most outstanding feature is the tripole structures in the stratosphere and tropopause: the positive

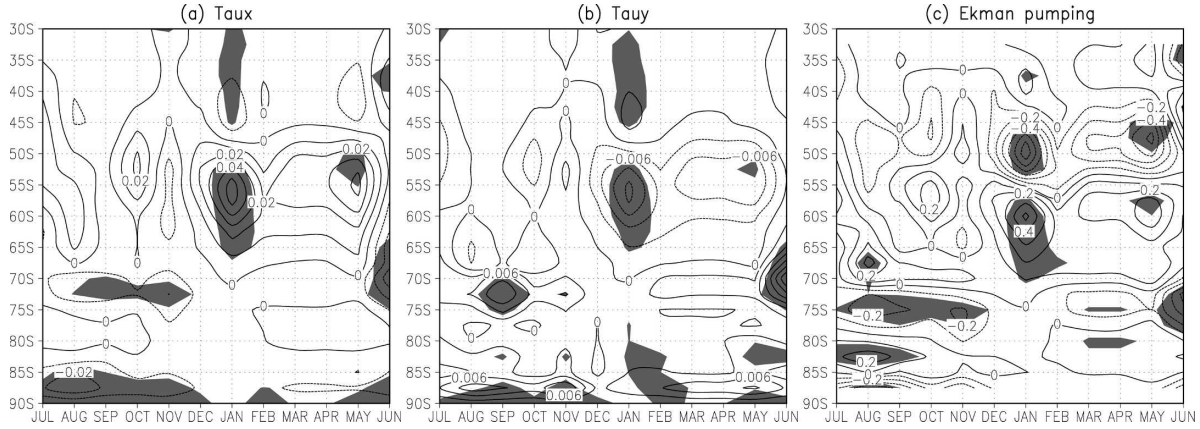

FIG. 2. Linear trends of each calendar month (1980–2000): (a) the zonal-mean zonal wind stress [unit: N m^{-2} (21 yr)$^{-1}$]; (b) the zonal-mean meridional wind stress (unit: N m^{-2}/21 yr); and (c) the Ekman pumping rate [unit: 10^{-6} m s^{-1} (21 yr)$^{-1}$]. Trends above the 95% significance level *t* test are shaded.

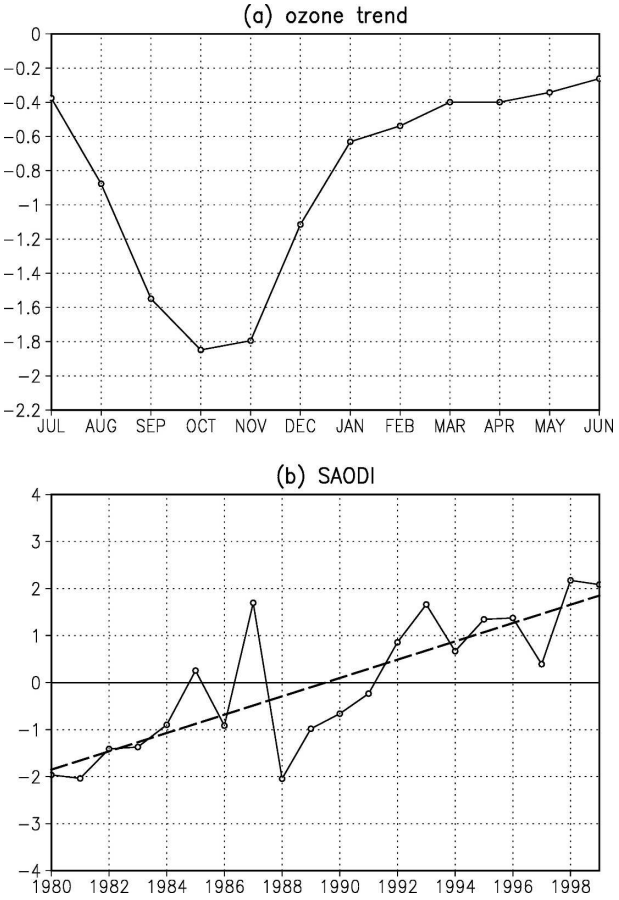

FIG. 3. (a) Linear trends of Antarctic (60°–90°S) total column ozone during 1980–99 [unit: 10^{-3} kg m^{-2} (20 yr)$^{-1}$]; (b) the SAODI time series (solid line) and its linear trend (dashed line).

correlations in the Antarctic stratosphere parallel negative correlations both at the Antarctic tropopause and in the midlatitude lower stratosphere. Previous studies revealed that the zones with sharp horizontal/vertical gradients of PV correspond to the positions of the polar vortex edge and tropopause (Hoskins 1991; Appenzeller and Davies 1992; Holton et al. 1995), where the planetary and synoptic-scale Rossby waves regularly "break" (McIntyre and Palmer 1984; Hoskins et al. 1985; Appenzeller et al. 1996; Polstel and Hitchman 1999). This correlation pattern results in the strengthening of PV gradients vertically and horizontally associated with spring Antarctic ozone depletion. The synchronously enhanced horizontal and vertical PV gradients in the lower-stratospheric Antarctic act to isolate the stratospheric polar region from the midlatitude and lower levels. Thus, more synoptic Rossby waves are refracted equatorward (Nakamura and Plumb 1994) and downward with less wave breaking and dynamical heating in the Antarctic, leading to a colder and stronger polar vortex (Figs. 4a,b) and the acceleration of circumpolar westerly winds (Fig. 4c). Since the ozone photochemical reaction is very sensitive to the environmental temperature, this situation further intensifies the Antarctic ozone depletion and favors a positive feedback loop.

In addition to the PV variations that are primarily caused by local synoptic wave forcing, ozone depletion also involves other nonlocal dynamical processes, which can be interpreted in terms of the upward Eliassen–Palm flux. Hood and Soukharev (2005) estimated that the two dynamical effects together can account for 50% of the observed negative trend of the column-integrated ozone and interannual variance at northern midlatitudes in late winter. The rest of the observed signals may be due to other physical factors, such as the anthropogenic influence. Polvani and Waugh (2004) reported that the eddy heat flux change in the lower stratosphere was always followed by anomalous polar vortex events. By numerical simulations, Scott and Polvani demonstrated that the upward flux of wave activity into the stratosphere strongly anticorrelates with the index of the mid–upper stratospheric vortex. Given the close linkage between stratospheric ozone, polar vortex, and upward eddy flux from troposphere into stratosphere, we computed the correlation coefficients between 30°–60°S averaged vertical EP flux and the SAODI (Fig. 6b). Here we choose the 30°–60°S band because the EP flux maximizes within this latitude range, as shown in its climatology (Fig. 6a). The significant negative correlation in the upper troposphere in spring and summer indicates a reduced wave forcing in accordance with ozone depletion.

So far, our analyses and calculations have been all based on the original data. As the apparent linear correlation of two variables may be strong by virtue of the shared trends (Thompson et al. 2000), we detrended both the SAODI and various physical variables and recalculated their regression coefficients (Fig. 7) and correlation coefficients (Fig. 8). The similarity between patterns in Fig. 4 and Fig. 7 testifies to the robustness of the previous statistical analyses. Nevertheless, there are discrepancies: detrended significant variations occur almost simultaneously with Antarctic ozone destruction in September–November rather than in a much broader time window from September to January, as diagnosed from the original data (Fig. 4). However, the spatial patterns of detrended correlation coefficients between temperature and the SAODI (Figs. 8a,b) as well as between PV and the SAODI (Figs. 8c,d) are all consistent with that of the original correlation (Fig. 5). This confirms the prolonged response of stratospheric circulation to the spring Antarctic ozone depletion in early

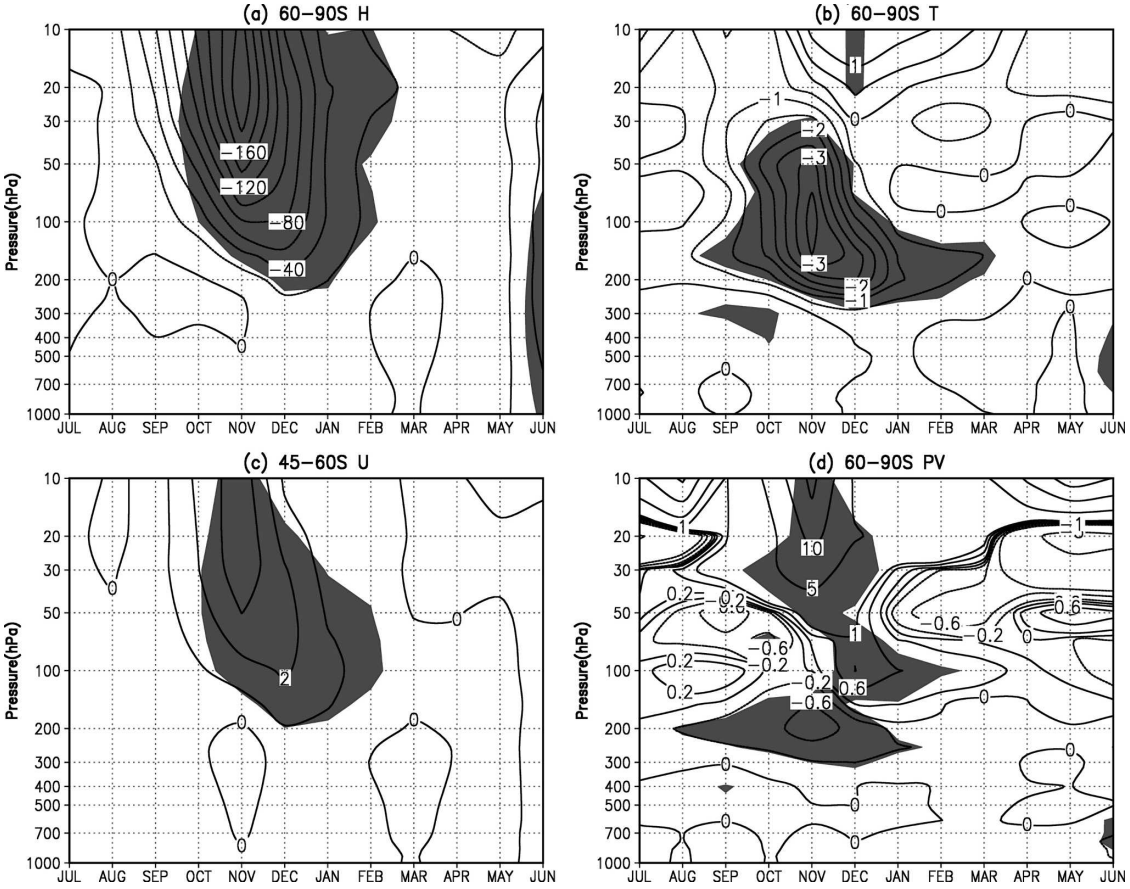

FIG. 4. Lag-regression coefficients on normalized SAODI. (a) Antarctic (60°–90°S) geopotential height (unit: m); (b) Antarctic air temperature (unit: K); (c) midlatitude (45°–60°S) zonal-mean zonal wind (unit: m s^{-1}); and (d) Antarctic PV (contour intervals: −15, −10, −5, −1, −0.6, −0.2, 0, 0.2, 0.6, 1, 5, 10, 15; unit: IPV, 1 IPV=10^{-6} K kg^{-1} m^2 s^{-1}). Shading denotes areas above the 95% significance level *t* test.

summer (December). Besides, the significant negative correlation between the SAODI and upward EP flux still exists in the lower stratosphere (August) and near tropopause (October and February), even though the trends are subtracted from both (Fig. 6c). This implies an ozone–eddy flux interaction process: Interannually, reduced upward eddy flux (and thus the poleward eddy heat flux) in early spring (August) contributes to the spring Antarctic ozone decline because a reduced poleward eddy heat flux favors a severe ozone depletion by the colder temperature. The Antarctic ozone depletion, in turn, causes a reduced midlatitude vertical EP flux in October and February. As Hu and Tung (2003) showed, decreasing upward wave activity is related to the enhancement of the equatorward wave reflection, and less eddy dynamical heating resulting from more wave refraction can be inferred as a component of the ozone-related feedback loop.

Now the ozone dynamics in the lower stratosphere can be roughly described as follows: the extraordinary spring Antarctic ozone depletion originates from the combined effect of human-released chemicals and the reduced upward wave flux in early spring. Then ozone depletion induces the intensification, stabilization, and cooling of the polar vortex with enhanced meridional gradients of PV and temperature between low and high latitudes, which further isolate the polar vortex and accelerate the circumpolar westerlies. At the same time, the strengthening of PV gradients vertically and horizontally refract more waves equatorward and downward to the troposphere, thus less dynamical heating and lower temperature in the lower stratosphere. In addition, the upward tropospheric eddy flux diminishes in accordance with the severe ozone depletion, resulting in less wave disturbances to the lower stratosphere and decreased poleward heat flux. This further favors a colder and more stable Antarctic polar vortex. The enhanced cooling renders the stratospheric ozone layer more susceptible to ozone-destroying chemicals (Austin et al. 1992; Shindell et al. 1998), hence more severe

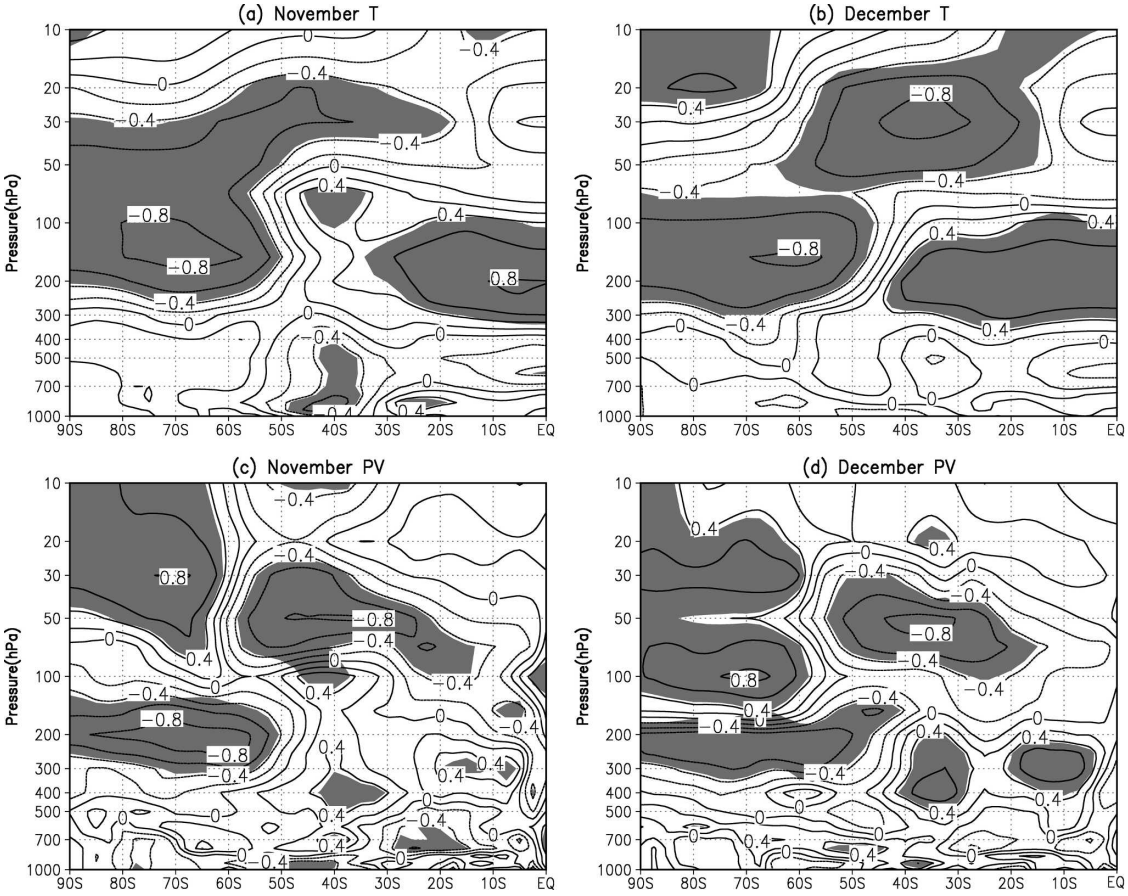

FIG. 5. Correlation between SAODI and zonal mean temperature during (a) November and (b) December. Correlation between SAODI and potential vorticity during (c) November and (d) December. Shading denotes areas above the 95% significance level *t* test.

ozone loss. This positive feedback contributes to the persistence of spring Antarctic ozone depletion and may be connected to the ozone-related long-term trends in austral summer.

Clear evidence of this idea can be found through the linear trend calculations (Fig. 9). Over the past two decades, the lower-stratosphere polar vortex has strengthened (Fig. 9a) and cooled (Fig. 9b), the mid-latitude westerly has accelerated (Fig. 9c), and 100-hPa Antarctic PV has increased (Fig. 9d). All of these trends are significant above the 95% confidence level in austral summer following the spring Antarctic ozone depletion, except that 200-hPa Antarctic PV (Fig. 9d) exhibits the significant downward trend in a rather broad time window from August to February. Besides, the Antarctic tropospheric temperature (Fig. 9b) has strong positive trends in winter and spring, which is assumed to be associated with greenhouse gas warming. The stratospheric trends tend to propagate downward to the lower troposphere, and the surface trends are significant in January only (Figs. 9a,c). The seasonality and structure of the 21-yr linear trend pattern of geopotential height (Fig. 9a) and temperature (Fig. 9b) are similar to that of the 30-yr observational trend pattern in TS02 (their Fig. 1) with a small discrepancy existing in the geopotential height amplitude.

Note that the linear trends of vertical EP flux exhibit the suppressed upward wave flux in the troposphere and increased upward wave flux in the lower stratosphere (Fig. 6d). Obviously, the correlation pattern (Figs. 6b,c) does support the consistency of spring ozone depletion with EP flux trends in the troposphere, but not in the lower stratosphere (the interannual correlation coefficients are not significant in the lower stratosphere). As the upward EP flux trends in the troposphere appear significant in austral winter and spring (June–November), it seems that the reduced tropospheric wave forcing trends lead the ozone depletion and then should have great dynamical effects on the ozone concentration. However, the lower-stratospheric

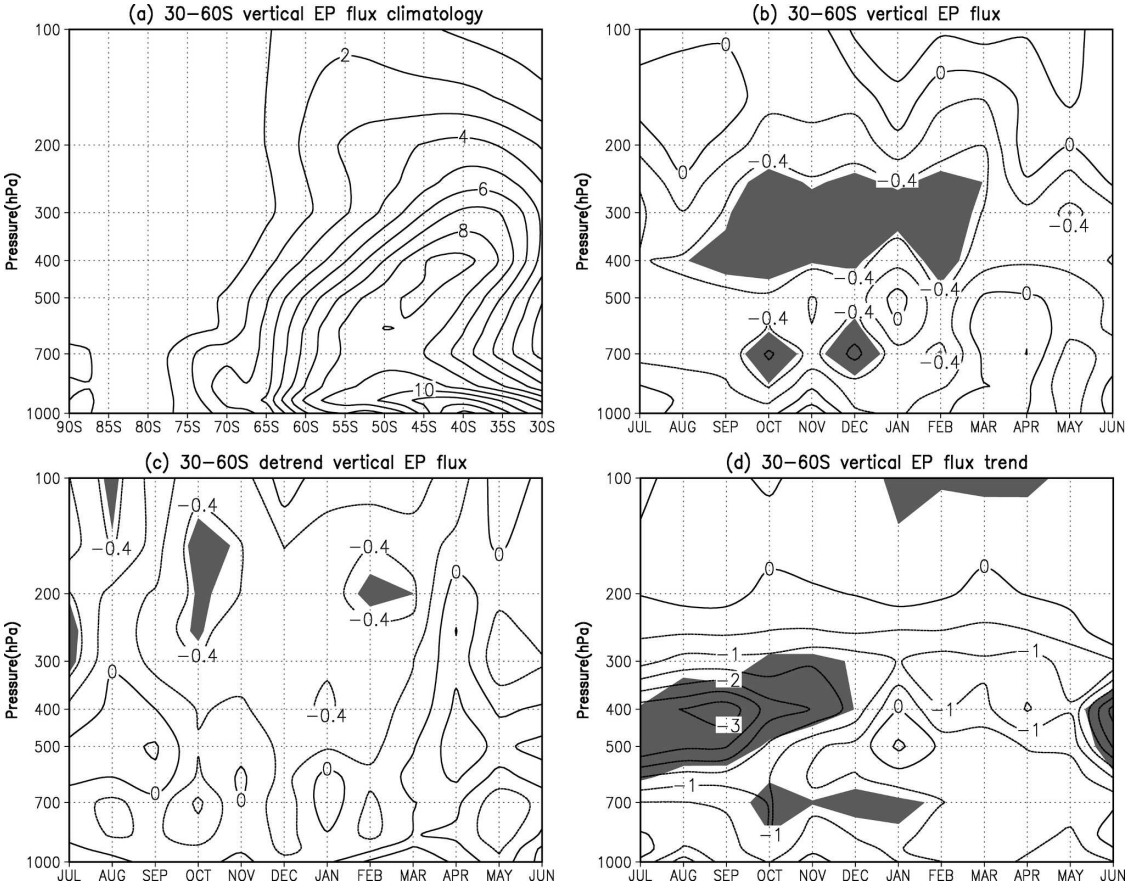

FIG. 6. (a) 30°–60°S vertical EP flux climatology; (b) correlation between 30°–60°S vertical EP flux and SAODI; (c) as in (b) but for detrended data; and (d) linear trends of 30°–60°S vertical EP flux. Shading denotes areas above the 95% significance level *t* test.

EP flux trends are independent of ozone dynamics, and the cause and effects of this phenomenon deserve more detailed investigation.

c. *The stratosphere–troposphere coupling and downward propagation of lower-stratospheric anomalies*

So far, we have depicted a positive feedback process in the lower stratosphere associated with spring Antarctic ozone depletion. Since our major interest is to find out how such anomalies can affect the sea level wind stress, we want to identify dynamical processes responsible for conveying these perturbations downward, that is, processes that generate the nonlocal effects of stratospheric ozone depletion. A potential candidate responsible for signal transport is the stratosphere–troposphere dynamical coupling.

It has been recognized that planetary Rossby waves generated in the troposphere can propagate upward. When their amplitude grows large enough, they break; their energy is absorbed and thus changes the stratospheric flow. The stratospheric flow, in turn, can affect the troposphere by downward wave refraction. Existing evidence indicates that the stratosphere–troposphere interaction processes can project onto the Southern Annular Mode in its active season (Thompson et al. 2000; Thompson and Solomon 2002; Thompson et al. 2005; Kushner and Polvani 2004). Accordingly, we construct 18-level SAM indices using ERA-40 monthly geopotential height data and investigate the downward propagation of zonal wind anomalies.

The SAM variabilities associated with the SAODI and its trends are shown in Fig. 10. Obviously, the decrease in Antarctic ozone concentration corresponds to the high polarity of SAM indices in the spring and summer stratosphere (Fig. 10a), and the SAM trends are strong and statistically significant in summer following the spring ozone depletion (Fig. 10c). Accordingly, the interannual correlations are largely reduced in summer, when the trends are subtracted from the ozone and SAM (Fig. 10b).

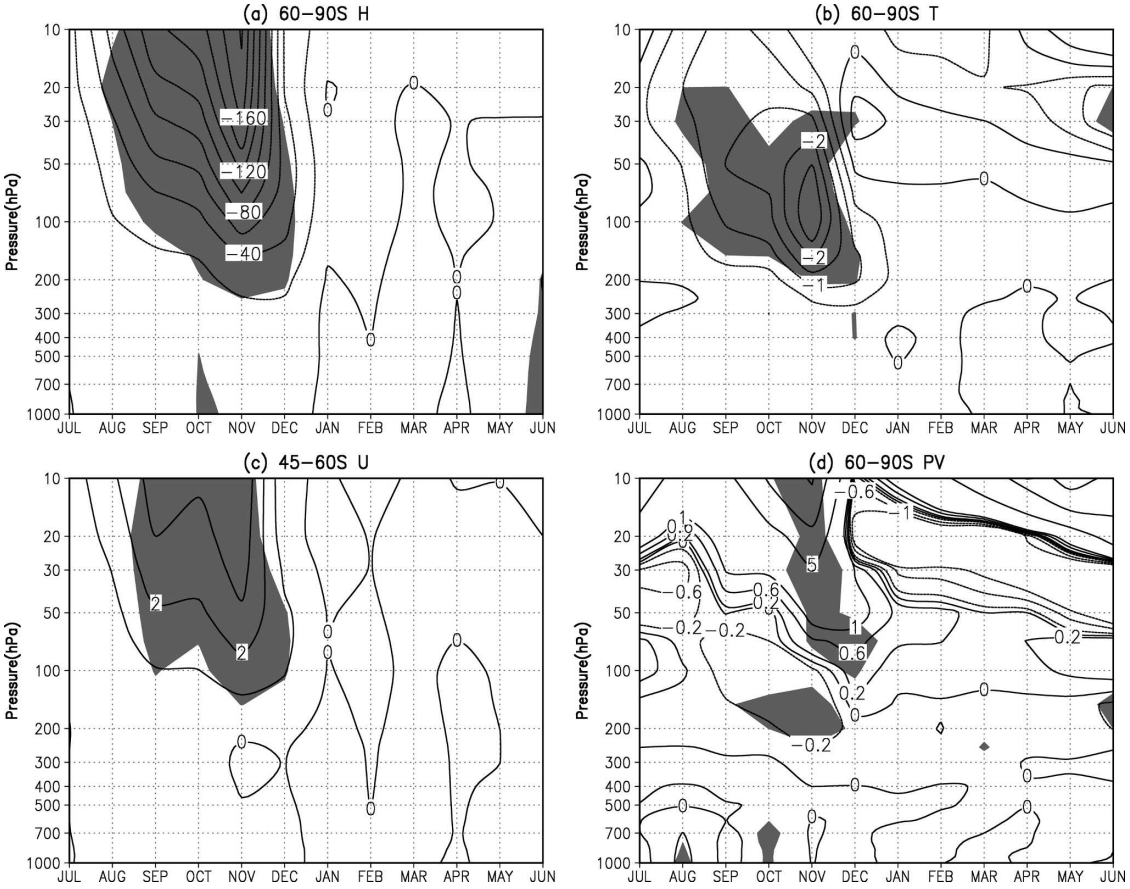

FIG. 7. As in Fig. 4 but for detrended data.

As noted in Baldwin et al. (2003a,b), the synoptic-scale baroclinic waves that originated from the instability of tropospheric flow may contribute to the apparent downward propagation of wind anomalies. The resulting wave–mean flow interaction drives the mean meridional circulation variations, which may be responsible for communicating the annular mode signals all the way to the surface (Baldwin and Dunkerton 2005). These previous studies inspired us to explore the interrelation of midlatitude wave activity variability, the corresponding zonal-mean meridional circulation, and the SAM. Figure 11 shows the correlation coefficients between the SAM indices and the SH midlatitude wave activity (EP flux). Positive values of the SAM are always accompanied by poleward eddy momentum transport, with maximum correlation occurring in austral winter (July), which accounts for the poleward shift and strengthening of the tropospheric westerly jet (Fig. 11a). On the other hand, correlations between the SAM and both the vertical EP flux (Fig. 11b) and the EP flux divergence (Fig. 11c) show a sandwichlike pattern in late spring/early summer (November–December). The positive phase of the SAM corresponds to reduced upward wave flux at the lower stratosphere–tropopause as well as in the lower troposphere, and the enhanced upward wave flux in the upper troposphere (Fig. 11b). Accordingly, the EP fluxes exhibit anomalous convergence in the upper troposphere (~300 hPa) and divergence in the lower stratosphere and lower troposphere (700–500 hPa; Fig. 11c). The EP flux divergence indicates the magnitude of zonal flow acceleration induced by wave activity (Edmon et al. 1980), with positive (negative) EP flux divergence indicating the westerly (easterly) acceleration (Limpasuvan and Hartmann 2000). Hence the high polarity of the SAM accounts for the enhancement of circumpolar westerlies in the lower stratosphere and at the same time promotes the downward spreading of anomalous westerly signals by the westerly deceleration in the upper troposphere and acceleration in the lower troposphere.

It has been widely recognized that vertical wave propagation can facilitate the stratosphere–troposphere coupling when the background zonal flow is westerly and below a threshold value (Charney and Drazin

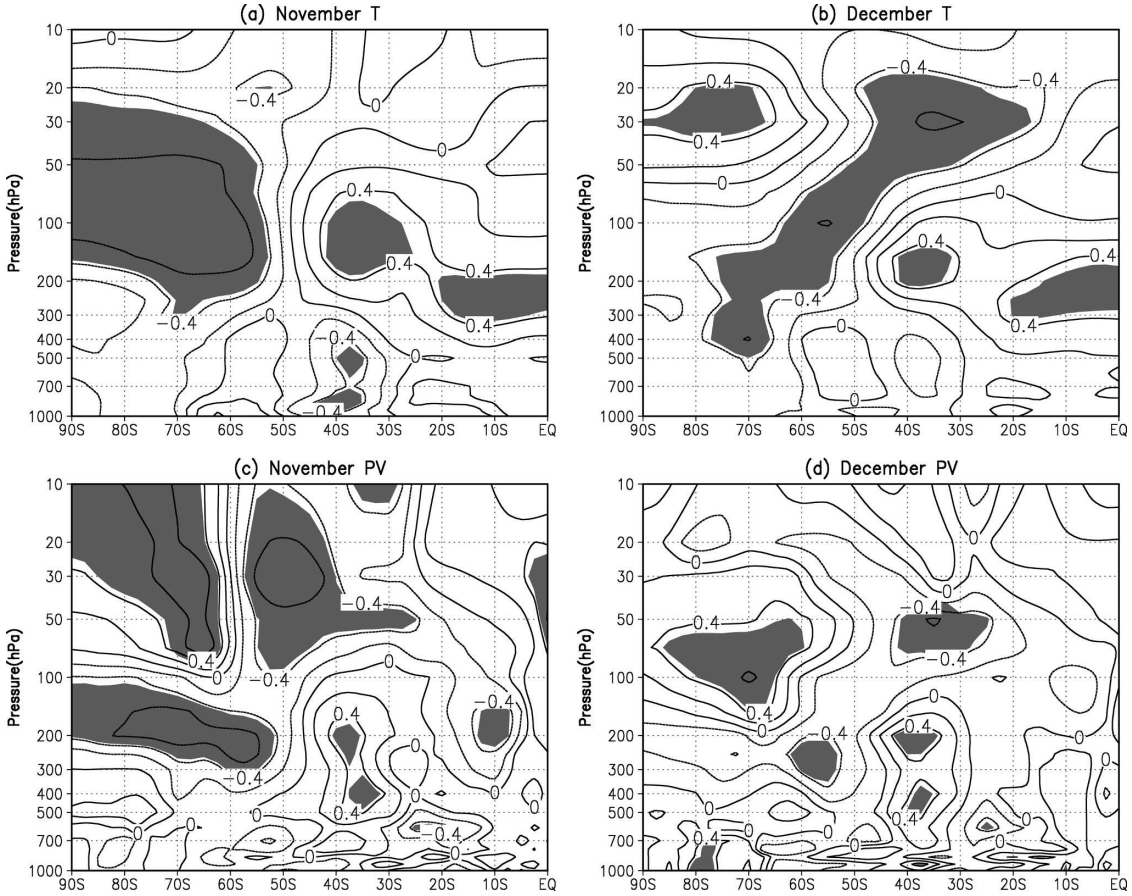

FIG. 8. As in Fig. 5 but for detrended data.

1961). This condition is met in the SH late spring/early summer when the polar vortex decays and when it is building up in the fall (Thompson and Solomon 2002). On account of the strong seasonality of the stratosphere–troposphere coupling and the lower-stratospheric circulation, we choose late spring/early summer (October–January) and present the zonal-mean meridional sections of eddy forcing (Fig. 12) and zonal-mean meridional circulation (Fig. 13) so as to ascertain the downward propagation of SAM-related zonal-wind anomalies. The late spring season (October–November) is characterized by prominent dipole patterns of EP flux divergence at midlatitudes (30°–60°S). The eddy fluxes converge at ~300 hPa and diverge at ~500 hPa, relaying the strong lower-stratospheric zonal-wind anomalies to the middle troposphere (Figs. 12a,b). In early summer (December–January), although the upper-level EP flux convergence diminishes to a large extent, the EP flux divergence at ~500 hPa persists, sustaining the strengthening of westerly wind at this level (Figs. 12c,d). On the other hand, the meridional Ferrel cell strengthens and shifts poleward in accordance with the positive phase of the SAM (vectors in Fig. 13). By virtue of the Coriolis force, the upper (lower-)-level branch of the Ferrel cell, that is, the anomalous southerly (northerly) winds, turns left to decelerate (accelerate) the anomalous westerlies, hence facilitating the downward propagation of westerly anomalies. At the same time, due to the SAM-related eddy momentum transport (Fig. 11a), the tropospheric westerly jet shifts poleward. The resulting coalescence of the tropospheric jet with the stratospheric polar night jet enhances the stratosphere–troposphere coupling and slows propagation of anomalous westerlies, thus collaborating to convey the SAM zonal-wind signals down to the surface, indicated by the downward shift of contours between October and January in Fig. 13.

4. Conclusions and discussion

Through a series of thermodynamical and dynamical interactions, the anthropogenic-induced spring Antarctic ozone depletion drives the decadal changes in the lower stratosphere and tropopause at the Southern

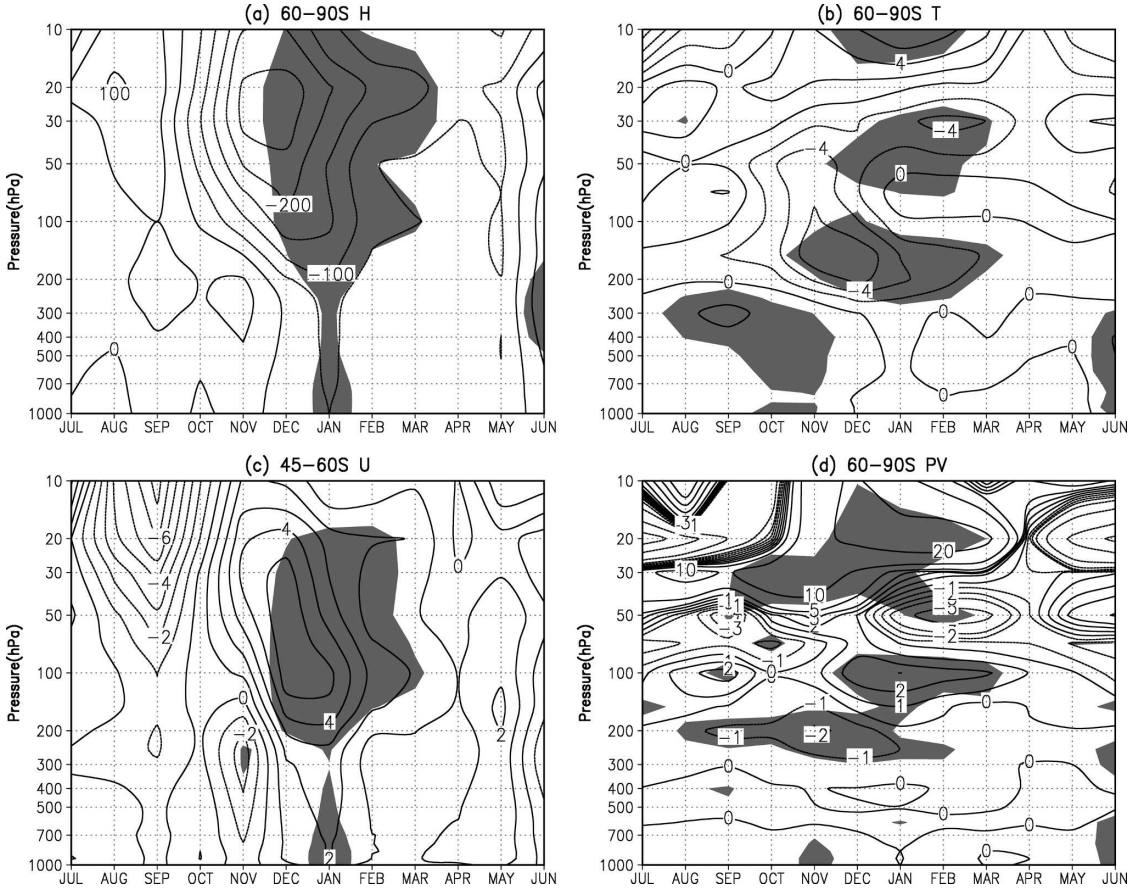

FIG. 9. As in Fig. 4 but for linear trends during the period of 1980–2000. [PV contour intervals in (d): −40, −30, −20, −10, −5, −3, −2, −1, 0, 1, 2, 3, 5, 10, 20, 30, 40.]

Hemisphere high and midlatitudes, as well as the high polarity of SAM in the austral spring and summer seasons. The stratosphere–troposphere coupling occurs during late spring–early summer by virtue of the SAM mode, resulting in the downward propagation of lower-stratospheric wind anomalies to the troposphere. It is the synergistic effect of SAM-related wave–mean flow interaction and anomalous mean meridional circulation that relays the wind anomaly signals and hereby triggers the positive trend of wind stress over the Southern Ocean.

The large-scale upper-level PV anomalies induce

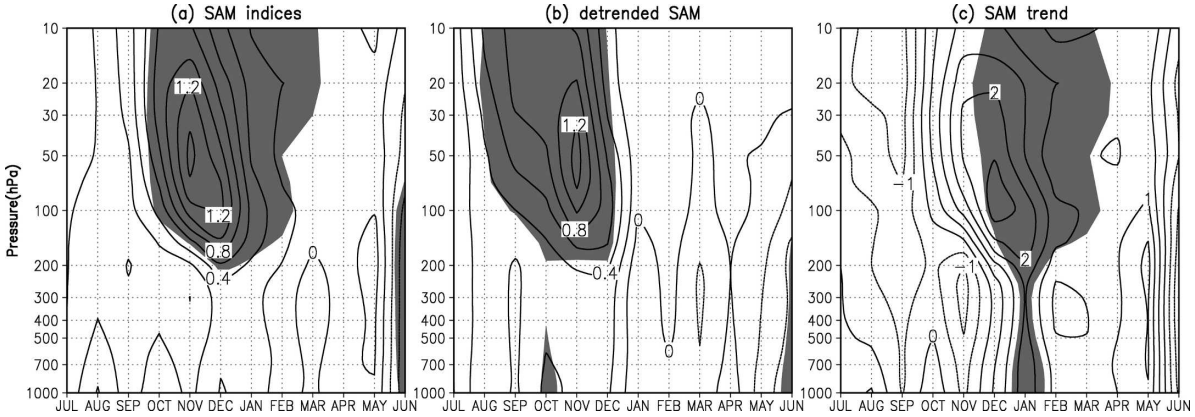

FIG. 10. (a) Lag-regression coefficients of SAM indices on SAODI; (b) as in (a) but for detrended data; and (c) linear trends of SAM indices for the period 1980–2000. Shading denotes areas above the 95% significance level *t* test.

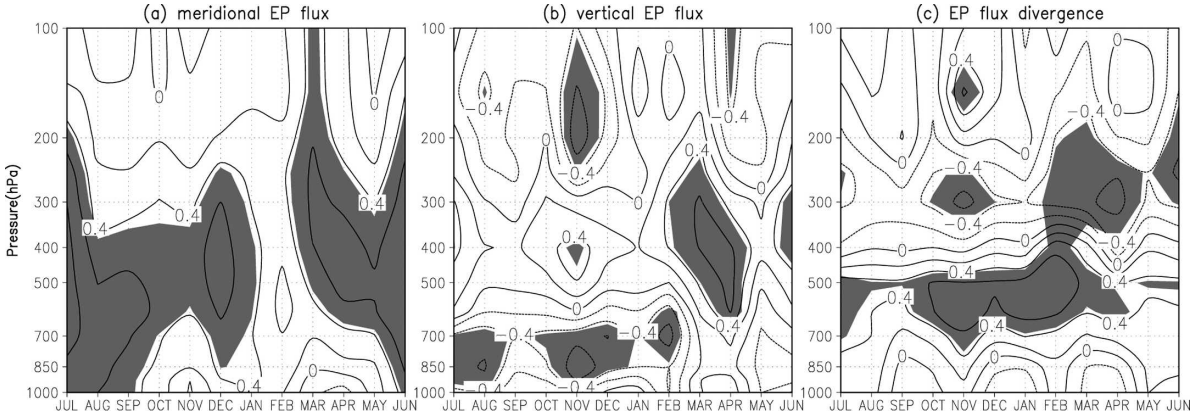

FIG. 11. Correlation between SAM indices and midlatitude (30°–60°S) EP flux: (a) the meridional EP flux; (b) the vertical EP flux; and (c) the EP flux divergence. Shading denotes areas above the 95% significance level *t* test.

strong wind fields that can be detected at the ground. By the method of piecewise potential vorticity inversion, both Hartley et al. (1998) and Black (2002) uphold the stratospheric downward forcing of tropospheric climate variability. Perlwitz and Harnik (2004), on the other hand, suggest that the downward reflection of waves is an important component of troposphere–stratosphere dynamics. Our analyses manifest the indi-

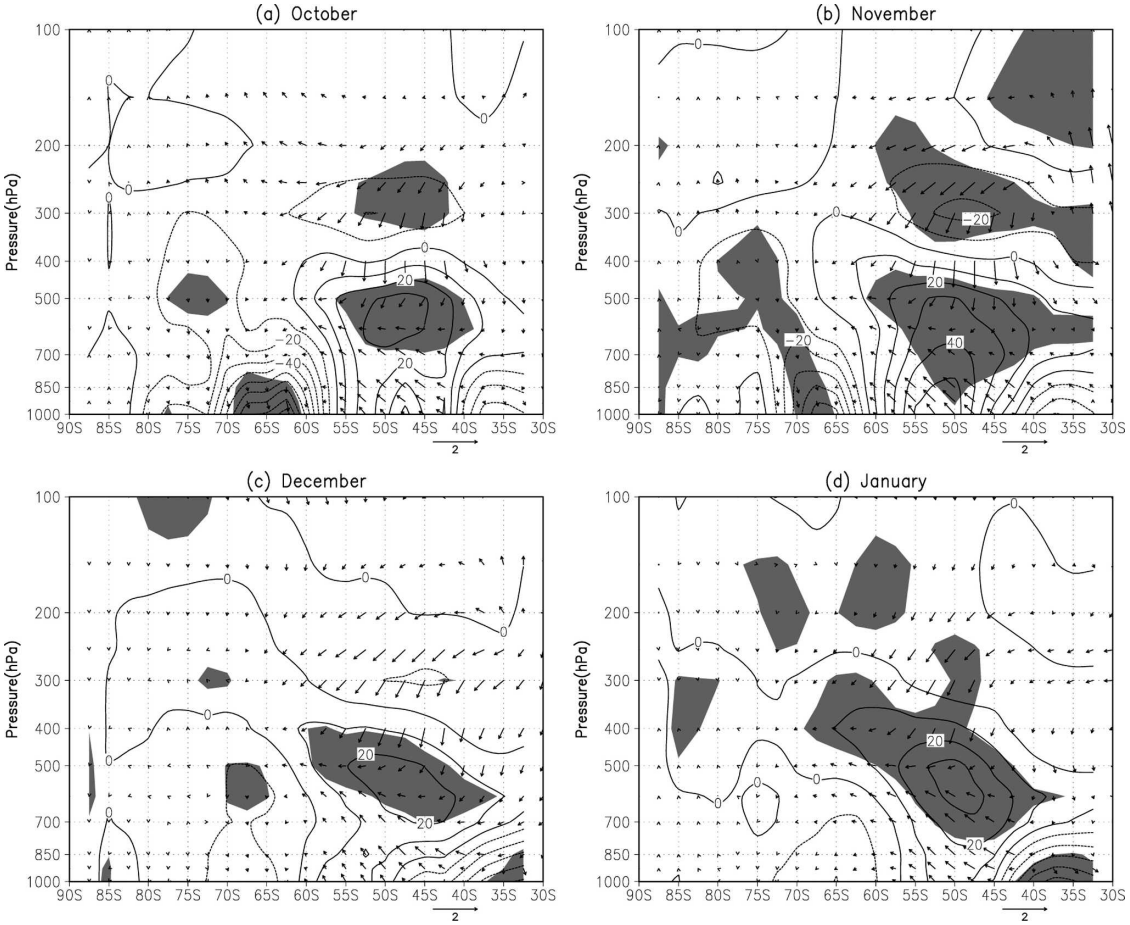

FIG. 12. Zonal-mean meridional sections of total EP fluxes (vector: the vertical component is multiplied by 200) and its divergences (contour) corresponding to one standard deviation of SAM indices. Shading denotes areas where the EP flux divergences are above the 95% significance level *t* test.

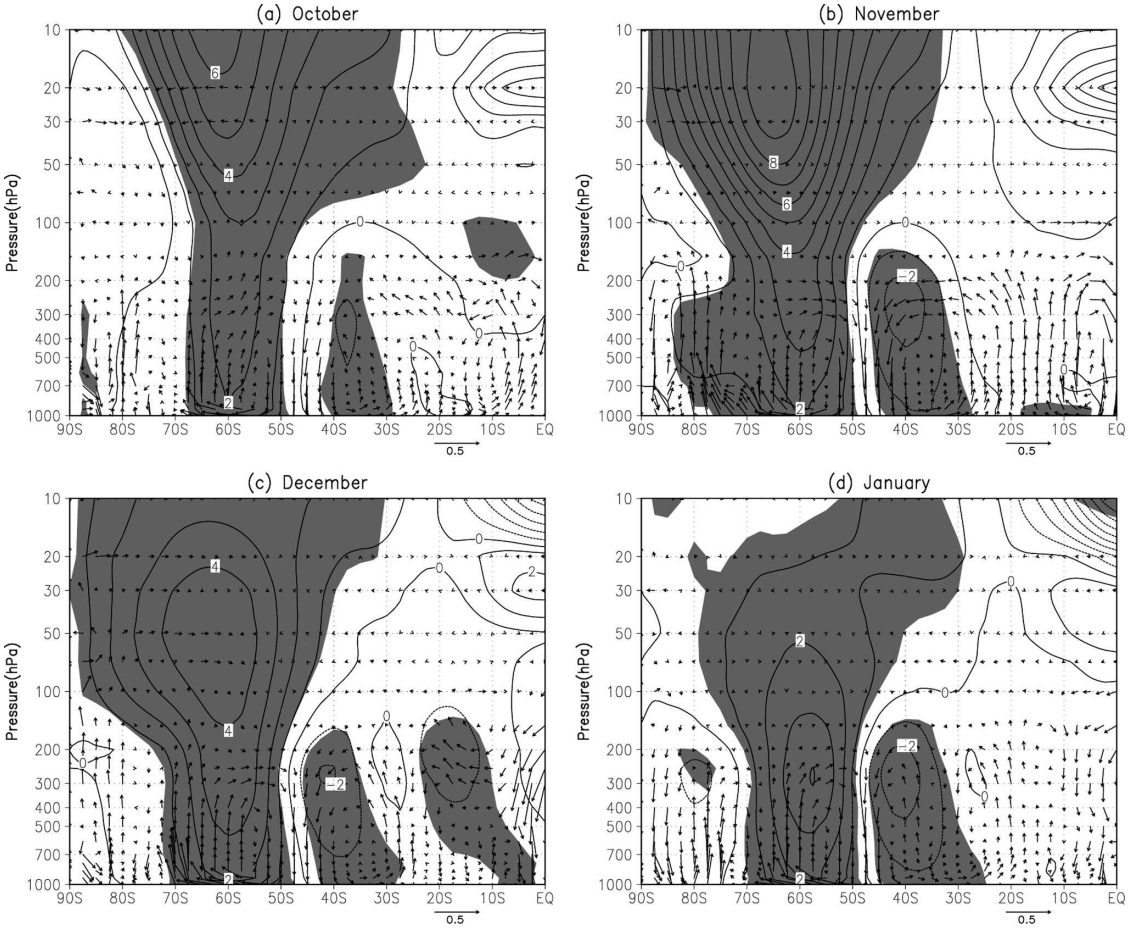

FIG. 13. Zonal-mean meridional circulation (vector: the vertical velocity is multiplied by 100) and zonal wind (contour) corresponding to one standard deviation of SAM indices. Shading denotes areas where the zonal wind anomalies are above the 95% significance level *t* test.

rect downward control of lower-stratospheric Antarctic ozone depletion on the Southern Ocean surface wind stress on decadal time scales. The ozone-related positive feedback influences the lower-stratospheric circulation and changes the tropospheric circulation through wave refraction, thus facilitating the stratosphere–troposphere coupling and downward propagation of zonal wind anomalies. This adds to the increasing number of studies (e.g., Baldwin et al. 2003b; Scott and Polvani 2004) that support the stratosphere as an active player in the stratosphere–troposphere interaction and thereby global climate changes.

Greenhouse gases (GHGs) have long been viewed as a principal factor driving climate changes (e.g., Fyfe et al. 1999; Kushner et al. 2001; Cai et al. 2003). The South Pole CO_2 monthly data (Fig. 1g) takes on a monotonic upward trend, and this linear trend persists for the whole 50-yr period in contrast to other time series. However, the seasonality and occurring period of Southern Ocean wind stress trends are highly coherent with the Antarctic ozone content. This implicates that at least in SH mid and high latitudes, the ozone hole plays a more important role than GHGs in driving the recent decadal variabilities, though their synergistic interactions should not be neglected (Hartmann et al. 2000; Shindell et al. 1998; Shindell and Schmidt 2004).

The importance of surface wind stress over the Southern Ocean in propelling the Antarctic Circumpolar Current (ACC) has been firmly established (Gnanadesikan and Hallberg 2000; Tansley and Marshall 2001; Borowski et al. 2002). Given the unique characteristics of ACC (zonally unblocked and huge transport capacity), the decadal change of the wind stress field will undoubtedly lead to considerable changes in the global ocean circulation.

Our discussion has been focused on the atmospheric dynamics; however, large-scale air–sea interaction in the Southern Ocean may also contribute to global cli-

mate changes. In particular, Antarctic Intermediate Water (AAIW) outcrops near the polar front where strong air–sea heat and momentum exchanges take place. In fact, recently reported Southern Ocean long-term variability associated with AAIW temperature and salinity property changes (e.g., Gille 2002) may be attributed to climate variabilities at its outcrop region. Changes in sea surface temperature and sea level wind stress may interact through complicated air–sea coupling mechanisms that, in turn, leads to the SH climate changes. Scientists have attempted to explore the ocean–atmospheric interaction in the Southern Ocean. Hall and Visbeck (2002) simulated the synchronous Southern Ocean changes corresponding to SAM. Oke and England (2004) presented the oceanic response to the latitudinal shifts of the subpolar westerly winds. More recently, Cai (2006) associated the southward shift and spinup of the supergyre in the Southern Ocean with surface wind changes induced by Antarctic ozone depletion. But the physical processes of the Southern Ocean in response to these ozone-induced changes may be far more complicated than commonly assumed. Thus, further inquiry of these processes may be pivotal to our comprehension of long-term ocean circulation and climate changes.

Acknowledgments. This study was supported by MOST of China (Grant 2006CB403604) and Chinese Academy of Sciences (Grant KZSW2-YW-214) (for YXY and DXW) and W. Alan Clark Chair from Woods Hole Oceanographic Institution (for RXH). Comments from the reviewers were very helpful in clearing up the presentation. The authors wish to thank Dr. Jason Goodman for his help in improving the quality of this manuscript and insightful comments. Discussions with Dr. Guihua Wang are much appreciated.

REFERENCES

Albritton, D. L., P. J. Aucamp, G. Megie, and R. T. Watson, 1998: Scientific Assessment of Ozone Depletion: 1998. Global Ozone Research and Monitoring Project, Rep. 44, World Meteorological Organization.

Appenzeller, C., and H. C. Davies, 1992: Structure of stratospheric intrusions into the troposphere. *Nature,* **358,** 570–572.

Appenzeller, E., J. R. Holton, and K. Rosenlof, 1996: Seasonal variation of mass transport across the tropopause. *J. Geophys. Res.,* **101,** 15 701–15 708.

Austin, J., N. Butchart, and K. Shine, 1992: Possibility of an Arctic ozone hole in a doubled-CO_2 climate. *Nature,* **360,** 221–225.

Baldwin, M. P., and T. J. Dunkerton, 2005: The solar cycle and stratosphere- troposphere dynamical coupling. *J. Atmos. Sol.-Terr. Phys.,* **67,** 71–82.

——, D. B. Stephenson, D. W. J. Thompson, T. J. Dunkerton, A. J. Charlton, and A. O'Neill, 2003a: Stratospheric memory and extended-range weather forecasts. *Science,* **301,** 636–640.

——, D. W. J. Thompson, E. F. Shuckburgh, W. A. Norton, and N. P. Gillett, 2003b: Weather from the stratosphere? *Science,* **301,** 317–319.

Bengtsson, L., K. I. Hodges, and S. Hagemann, 2004: Sensitivity of the ERA40 reanalysis to the observing system: Determination of the global atmospheric circulation from reduced observations. *Tellus,* **56A,** 456–471.

Black, R. X., 2002: Stratospheric forcing of surface climate in the Arctic Oscillation. *J. Climate,* **15,** 268–277.

Borowski, D., R. Gerdes, and D. Olbers, 2002: Thermohaline and wind forcing of a circumpolar channel with blocked geostrophic contours. *J. Phys. Oceanogr.,* **32,** 2520–2540.

Cai, W., 2006: Antarctic ozone depletion causes an intensification of the Southern Ocean super-gyre circulation. *Geophys. Res. Lett.,* **33,** L03712, doi:10.1029/2005GL024911.

——, P. H. Whetton, and D. J. Karoly, 2003: The response of the Antarctic Oscillation to increasing and stabilized atmospheric CO_2. *J. Climate,* **16,** 1525–1538.

Charney, J. G., and P. G. Drazin, 1961: Propagation of planetary-scale disturbances from the lower into the upper atmosphere. *J. Geophys. Res.,* **66,** 83–109.

Chung, C., and S. Nigam, 1999: Weighting of geophysical data in Principal Component Analysis. *J. Geophys. Res.,* **104,** 16 925–16 928.

Crutzen, P. J., and F. Arnold, 1986: Nitric-acid cloud formation in the cold Antarctic stratosphere: A major cause for the springtime ozone hole. *Nature,* **324,** 651–655.

Edmon, H. J., Jr., B. J. Hoskins, and M. E. McIntyre, 1980: Eliassen–Palm cross sections for the troposphere. *J. Atmos. Sci.,* **37,** 2600–2616.

Farman, J. C., B. G. Gardiner, and J. D. Shankin, 1985: Large losses of total ozone in Antarctica reveal ClOX/NOX interaction. *Nature,* **315,** 207–210.

Fyfe, J. C., G. J. Boer, and G. M. Flato, 1999: The Arctic and Antarctic oscillations and their projected change under global warming. *Geophys. Res. Lett.,* **26,** 1601–1604.

Garratt, J. R., 1977: Review of drag coefficients over oceans and continents. *Mon. Wea. Rev.,* **105,** 915–929.

Gille, S. T., 2002: Warming of the Southern Ocean since the 1950s. *Science,* **295,** 1275–1277.

Gillett, N. P., and D. W. J. Thompson, 2003: Simulation of recent Southern Hemisphere climate change. *Science,* **302,** 273–275.

Gnanadesikan, A., and R. W. Hallberg, 2000: On the relationship of the circumpolar current to the Southern Hemisphere winds in the coarse-resolution ocean models. *J. Phys. Oceanogr.,* **30,** 2013–2034.

Hall, A., and M. Visbeck, 2002: Synchronous variability in the Southern Hemisphere atmosphere, sea ice, and ocean resulting from the Annular Mode. *J. Climate,* **15,** 3043–3057.

Hartley, D. E., J. Villarin, R. X. Black, and C. A. Davis, 1998: A new perspective on the dynamical link between the stratosphere and troposphere. *Nature,* **391,** 471–474.

Hartmann, D. L., J. M. Wallace, V. Limpasuvan, D. W. J. Thompson, and J. R. Holton, 2000: Can ozone depletion and global warming interact to produce rapid climate change? *Proc. Natl. Acad. Sci. USA,* **92,** 1412–1417.

Hines, K. M., D. H. Bromwich, and G. J. Marshall, 2000: Artificial surface pressure trends in the NCEP–NCAR reanalysis over the Southern Ocean and Antarctica. *J. Climate,* **13,** 3940–3952.

Holton, J. R., P. H. Haynes, M. E. McIntyre, A. R. Douglass, R. B. Rood, and L. Pfister, 1995: Stratosphere-troposphere exchange. *Rev. Geophys.,* **33,** 403–439.

Hood, L. L., and B. E. Soukharev, 2005: Interannual variations of total ozone at northern midlatitudes correlated with stratospheric EP flux and potential vorticity. *J. Atmos. Sci.,* **62,** 3724–3739.

Hoskins, B. J., 1991: Towards a PV-θ view of the general circulation. *Tellus,* **43AB,** 27–35.

——, M. E. McIntyre, and A. W. Robertson, 1985: On the use and significance of isentropic potential vorticity maps. *Quart. J. Roy. Meteor. Soc.,* **111,** 877–946.

Hu, Y. Y., and K. K. Tung, 2003: Possible ozone-induced long-term changes in planetary wave activity in late winter. *J. Climate,* **16,** 3027–3038.

Huang, R. X., 1998: On the balance of energy in the oceanic general circulation. *Chin. J. Atmos. Sci,* **22,** 452–467.

——, 2004: Ocean, energy flow. *Encyclopedia of Energy,* C. J. Cleveland, Ed., Vol. 4, Elsevier, 497–509.

——, W. Wang, and L. L. Liu, 2006: Decadal variability of wind energy input to the world ocean. *Deep-Sea Res. II,* **53,** 31–41.

Kallberg, P., A. Simmons, S. Uppala, and M. Fuentes, 2004: The ERA-40 archive. ERA-40 Project Report Series No. 17, 35 pp.

Kushner, P. J., and L. M. Polvani, 2004: Stratosphere–troposphere coupling in a relatively simple AGCM: The role of eddies. *J. Climate,* **17,** 629–639.

——, I. M. Held, and T. L. Delworth, 2001: Southern Hemisphere atmospheric circulation response to global warming. *J. Climate,* **14,** 2238–2249.

Langematz, U., 2000: An estimate of the impact of observed ozone losses on stratospheric temperature. *Geophys. Res. Lett.,* **27,** 2077–2080.

Limpasuvan, V., and D. L. Hartmann, 2000: Wave-maintained annular modes of climate variability. *J. Climate,* **13,** 4414–4429.

Mahlmann, R. D., J. P. Pinto, and L. J. Umscheid, 1994: Transport, radiative, and dynamical effects of the Antarctic ozone hole: A GFDL "SKYHI" model experiment. *J. Atmos. Sci.,* **51,** 489–509.

Marshall, G. J., 2002: Trends in Antarctic geopotential height and temperature: A comparison between radiosonde and NCEP–NCAR reanalysis data. *J. Climate,* **15,** 659–674.

——, 2003: Trends in the southern annular mode from observations and reanalyses. *J. Climate,* **16,** 4134–4143.

McElroy, M. B., R. J. Salawitch, S. C. Wofsy, and J. A. Logan, 1986: Reductions of Antarctic ozone due to synergistic interactions of chlorine and bromine. *Nature,* **321,** 759–762.

McIntyre, M. E., and T. N. Palmer, 1984: The "surf zone" in the stratosphere. *J. Atmos. Terr. Phys.,* **46,** 825–849.

Nakamura, M., and R. A. Plumb, 1994: The effects of flow asymmetry on the direction of Rossby wave breaking. *J. Atmos. Sci.,* **51,** 2031–2045.

Oke, P. R., and M. H. England, 2004: Ocean response to changes in the latitude of the Southern Hemisphere subpolar westerly winds. *J. Climate,* **17,** 1040–1054.

Perlwitz, J., and N. Harnik, 2004: Downward coupling between the stratosphere and troposphere: The relative roles of wave and zonal mean processes. *J. Climate,* **17,** 4902–4909.

Polstel, G. A., and M. H. Hitchman, 1999: A climatology of Rossby wave breaking along the subtropical tropopause. *J. Atmos. Sci.,* **56,** 359–373.

Polvani, L. M., and D. W. Waugh, 2004: Upward wave activity flux as a precursor to extreme stratospheric events and subsequent anomalous surface weather regimes. *J. Climate,* **17,** 3548–3554.

Ramaswamy, V., and Coauthors, 2001: Stratospheric temperature trends: Observations and model simulations. *Rev. Geophys.,* **39,** 71–122.

Randel, W. J., and F. Wu, 1999: Cooling of the Arctic and Antarctic polar stratospheres due to ozone depletion. *J. Climate,* **12,** 1467–1479.

Santer, B. D., T. M. L. Wigley, J. S. Boyle, D. J. Gaffen, J. J. Hnilo, D. Nychka, D. E. Parker, and K. E. Taylor, 2000: Statistical significance of trends and trend differences in layer-average atmospheric temperature time series. *J. Geophys. Res.,* **105,** 7337–7356.

Scott, R. K., and L. M. Polvani, 2004: Stratospheric control of upward wave flux near the tropopause. *Geophys. Res. Lett.,* **31,** L02115, doi:10.1029/2003GL017965.

Shindell, D. T., and G. A. Schmidt, 2004: Southern Hemisphere climate response to ozone changes and greenhouse gas increases. *Geophys. Res. Lett.,* **31,** L18209, doi:10.1029/2004GL020724.

——, D. Rind, and P. Lonergan, 1998: Increased polar stratospheric ozone losses and delayed eventual recovery due to increasing greenhouse gas concentrations. *Nature,* **392,** 589–592.

Shine, K. P., 1986: On the modeled thermal response of the Antarctic stratosphere to a depletion of ozone. *Geophys. Res. Lett.,* **13,** 1331–1334.

Solomon, S., 1999: Stratospheric ozone depletion: A review of concepts and history. *Rev. Geophys.,* **37,** 275–316.

——, R. R. Garcia, F. S. Rowland, and D. J. Wuebbles, 1986: On the depletion of Antarctic ozone. *Nature,* **321,** 755–758.

Stolarski, R. S., A. J. Krueger, M. R. Schoeberl, R. D. McPeters, P. A. Newman, and J. C. Alpert, 1986: Nimbus-7 satellite measurements of the springtime Antarctic ozone decrease. *Nature,* **322,** 808–811.

Tansley, C. E., and D. P. Marshall, 2001: On the dynamics of wind-driven circumpolar currents. *J. Phys. Oceanogr.,* **31,** 3258–3273.

Thompson, D. W. J., and S. Solomon, 2002: Interpretation of recent Southern Hemisphere climate change. *Science,* **296,** 895–899.

——, J. M. Wallace, and G. C. Hegerl, 2000: Annular modes in the extratropical circulation. Part II: Trends. *J. Climate,* **13,** 1018–1036.

——, M. P. Baldwin, and S. Solomon, 2005: Stratosphere–troposphere coupling in the Southern Hemisphere. *J. Atmos. Sci.,* **62,** 708–715.

Waugh, D. W., W. J. Randel, S. Pawson, P. A. Newman, and E. R. Nash, 1999: Persistence of the lower stratospheric polar vortices. *J. Geophys. Res.,* **104,** 27 191–27 201.

Wunsch, C., and R. Ferrari, 2004: Vertical mixing, energy, and the general circulation of the oceans. *Annu. Rev. Fluid Mech.,* **36,** 281–314.

Zhou, S., M. E. Gelman, A. J. Miller, and J. P. McCormack, 2000: An inter-hemisphere comparison of the persistent stratospheric polar vortex. *Geophys. Res. Lett.,* **27,** 1123–1126.